

See discussions, stats, and author profiles for this publication at: <https://www.researchgate.net/publication/51098338>

Thermal Stability and Structural Variations of Survivin and Its Deletants in Aqueous Solution as Revealed by Spectroscopy

ARTICLE in THE JOURNAL OF PHYSICAL CHEMISTRY B · JUNE 2011

Impact Factor: 3.3 · DOI: 10.1021/jp200060q · Source: PubMed

CITATIONS

23

READS

39

7 AUTHORS, INCLUDING:



Huafei Zhang

Jilin University

6 PUBLICATIONS 53 CITATIONS

SEE PROFILE



Xianghui Yu

Jilin University

59 PUBLICATIONS 1,913 CITATIONS

SEE PROFILE



Xiao Zha

Sichuan Tumor Hospital and Institute

41 PUBLICATIONS 668 CITATIONS

SEE PROFILE



Yuqing Wu

Jilin University

124 PUBLICATIONS 1,696 CITATIONS

SEE PROFILE

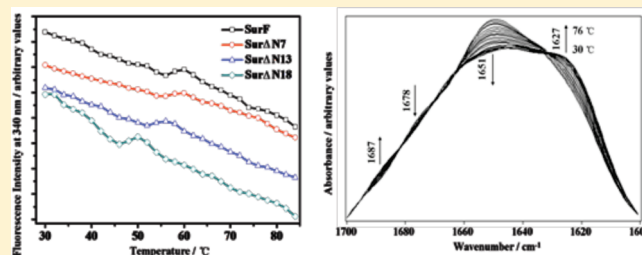
Thermal Stability and Structural Variations of Survivin and Its Deletants in Aqueous Solution as Revealed by Spectroscopy

Yang Gao,[†] Min Zhang,[†] Huafei Zhang,[‡] Xianghui Yu,[‡] Wei Kong,[‡] Xiao Zha,[§] and Yuqing Wu^{*,†}[†]State Key Laboratory for Supramolecular Structure and Materials and [‡]State Engineering Laboratory of AIDS Vaccine, Jilin University, No. 2699, Qianjin Street, Changchun 130012 China[§]Sichuan Tumor Hospital & Institute, Chengdu 610041 China

S Supporting Information

ABSTRACT: Survivin exists as a homodimeric conformation to act as a suppressor of apoptosis in organisms. Previously, we found that the deletants with truncations of N-terminal residues up to Arg18 lost the binding ability to Smac/DIABLO but not the binding force of homodimers. In order to establish the relationship between function and structural stability, thermal unfolding of SurF and its deletants in buffer have been studied in the present paper. The fluorescent results indicated that with the removal of the N-terminus, the thermal stability of the tertiary structure dropped vigorously, especially for Sur Δ N18.

However, using circular dichroism (CD) spectroscopy, we observed that the main unfolding of the secondary structures was not affected very much with N-terminus deletion. Fourier transform infrared (FT-IR) spectroscopy and two-dimensional (2D) correlation analysis were further used to provide structural information that occurred in the main transitions, which were associated with conformational changes of several β -components and α -helix, followed by the gain of some aggregations and random coils at high temperature. In addition, more aggregates were found to form for the longer N-terminal deletants during the main unfolding.



INTRODUCTION

Survivin is the smallest member of the inhibitor of the apoptosis protein (IAP) family and is selectively expressed in the G2/M phase of a cell cycle. It has dual functions; on one hand, it acts as a suppressor of apoptosis, and on the other hand, it plays a pivotal role in cell division.^{1,2} Survivin is overexpressed in most human neoplasms, embryos, and malignant tissues but not in normal tissues.^{3,4} Detection of Survivin has prognostic relevance for some tumor cells. In addition, it appears to be involved in their resistance to anticancer agents and ionizing radiation. As a consequence, all of that makes this protein a novel target for cancer therapy.^{5–7}

Not only the structure of Survivin is distinctive but also the function of it is complicated. Its monomer is a 16.5 kDa protein containing 142 amino acids and structurally consists of an N-terminal single globular baculovirus IAP repeat (BIR) domain (M1–S88), a linker segment (V89–T97), and a long amphipathic C-terminal coiled-coil α -helix (L98–D142).⁸ Simultaneously, a three-stranded β -sheet and four α -helices containing a zinc-binding fold, which is similar to that found in the XIAP (X-linked IAP) BIR2 and BIR3 domains including the structure formed by three Cys, one His, and a zinc ion, composed the Survivin BIR domain,⁹ but it lacked the RING finger motif found in XIAP. On the basis of both X-ray crystal diffraction^{10,11} and NMR spectroscopy¹² in solution, Survivin exists in two unparallel forms which correlate with its different functions in vivo. First, the chromosomal

passenger complex (CPC), which interacts with Aurora-B kinase as a key regulator of chromosome segregation and cytokinesis during the cell cycle, is formed by the monomer of Survivin associating with Borealin and INCENP (inner centromere protein). Therefore, the monomer of Survivin participates in the cell division directly.^{10,13,14} Second, in the antiapoptosis state, Survivin exists as a bow-tie-shaped homodimer, and the dimer interface, which involves both residues 6–13 in the N-terminal portion and a 14 amino acid region encompassing residues 89–102 located just in and after the linker segment, is significantly extensive.^{8,11,12} The hydrophobic interaction was mainly dominated by the interaction surface formed by Leu98 protruding from one monomer and extending into a hydrophobic pocket formed by Leu6, Trp10, Phe93, Phe101, and Leu102 in the other monomer molecule, which is of significance for the dimer formation and for the stability of the protein as well.

Over the past decades, much effort has been devoted to understanding the mechanisms of the protein unfolding problem and the structure–function relationship, which will help to perform the modification and design of novel proteins or peptide mimetics.^{15,16} Detailed investigation of the structure of the protein in the unfolded state has been a major research topic in the

Received: January 4, 2011

Revised: March 26, 2011

Published: May 04, 2011

field of protein chemistry and biophysics in recent years^{17–19} and can play crucial roles in bio- and nanotechnology. Furthermore, two-dimensional correlation infrared spectroscopy is very powerful to unravel the highly complicated infrared bands of proteins.^{20,21} In variable–variable (VV) 2D correlation spectroscopy, it enables one to establish the correlation between different secondary structures of the protein through selective correlation peaks for a given perturbation. This provides detailed information on the process under investigation, including the sequence of events and the possibility of band assignments.^{22–24} Its application simplifies the investigation of complex spectra consisting of many overlapping bands and enhances spectral resolution by spreading peaks along the second dimension, enabling one to extract information that cannot be obtained straightforwardly from one-dimensional spectra.

In the previous work,²⁵ we constructed and purified full-length human Survivin (SurF) and a series of its deletants from *Escherichia coli*, Sur Δ N7 (truncated 7 N-terminal residues), Sur Δ N13 (truncated 13 N-terminal residues), and Sur Δ N18 (truncated 18 N-terminal residues), and made sure that they all could fold in a right way and still dimerize in solution. We quantitatively evaluated the contribution of the N-terminal sequences on the strength of the dimerization by using single-molecule force spectroscopy (SMFS) and the binding ability to Smac/DIABLO in vitro. The results revealed that the N-terminal residues up to Arg18 were not essential for dimerization, but the binding of them to Smac/DIABLO determined by ELISA was strongly dependent on the length of N-terminal deletions; Sur Δ N7 was as efficient as the wild-type SurF, but that of Sur Δ N13 was significantly reduced, and that of Sur Δ N18 was completely lost. Together, these findings provide direct evidence that the N-terminal sequence of Survivin is not critical for dimer formation but may contribute to its correct folding and BIR function. As residues 1–18 were not the reported binding sites to Smac/DIABLO,¹² the large differences between Survivin deletants may result from their tertiary structural distinction. Therefore, to establish the relationship between function and structure, investigation of the thermal stability and structural variation of SurF and the deletants becomes necessary.

In this study, we investigated the thermal-induced structural changes, including both tertiary and secondary conformational transition of the four dimeric Survivins were studied in buffer solutions using fluorescence, circular dichroism (CD), and Fourier transform infrared (FT-IR) spectroscopy. The target was to explore the contribution of the N-terminal residues to the whole molecule thermal stability of human Survivin. Meanwhile, the drastic structural transitions, especially the subtle structural variations of proteins, have been revealed well by using the VV 2D correlation analysis. The obtained results offer a representation with the molecular explanation of what happens to the structure of human Survivin with N-terminal deletion at high temperatures.

MATERIALS AND METHODS

Protein Production. A 6 \times His affinity tag was placed at the C-terminal of human Survivin and the deletants by PCR using specific primers. The fused cDNAs were subcloned into the T7 expression vector pRSETB (amp^r; Invitrogen, Carlsbad, CA) for the NdeI and HindIII (Takara Bio Inc., Otsu, JP) multiclonal site, and the expression of the protein was made in *E. coli* BL21-DE3 cells (Novagen, Germany). The purification of the protein was

obtained by a nickel affinity column (0.5 mL of resin/L of culture; GE Healthcare Biosciences, PA) according to the manufacturer's instructions, followed by renaturation of the deletants by dialyses and desalination by a second chromatographic step on the Sephadex G-25 Medium (PD-10 desalting column, GE Healthcare Biosciences, PA). The purity of SurF and that of the deletants were determined by SDS-PAGE (see Supporting Information, Figure S1) and Western blotting,²⁵ and the protein concentrations were calculated based on the BCA protein assay kit (BIPEC Bioreagent, Bipec Biopharma Corporation, Cambridge, MA) and measured the absorbance values at 562 nm.

Thermal-Dependent Fluorescence Spectroscopy. The emission spectra of the intrinsic tryptophane fluorescence were measured on a computer-controlled Shimadzu RF-5301PC fluorescence spectrofluorometer (Tokyo, Japan) equipped with a circulating thermostatic bath (Shanghai, China) using 1 cm quartz cells with an excitation wavelength of 280 nm. The solutions containing SurF and the deletants were prepared with a concentration of 20 μ g/mL in PBS buffer (20 mM phosphate buffer solution containing 100 mM NaCl and 50 μ M Zn²⁺, pH 8.0), and the emission spectra were measured in the temperature range of 30.0–84.0 $^{\circ}$ C with an increment of 2.0 $^{\circ}$ C. During all measurements, a constant temperature in the sample holder was maintained by an external bath circulator and carefully checked by a thermocouple. Each spectrum was measured after the sample had been equilibrated for 10 min at an expected temperature. For each case, three independent fluorescence measurements were performed for each protein after the protein was newly prepared, and the representative data were presented.

Thermal-Dependent Circular Dichroism Spectroscopy. Far-UV CD spectra were obtained on a Jasco J-810 spectrophotometer (Tokyo, Japan) using a 1 cm path length. The solutions containing SurF and the deletants were prepared with a concentration of 100 μ g/mL in PBS buffer above.²⁶ The CD spectra of the protein solution were measured in the temperature range of 30.0–80.0 $^{\circ}$ C with an increment of 2.0 $^{\circ}$ C. During all measurements, a constant temperature in the sample holder was maintained by a circulating thermostatic bath (Shanghai, China) and carefully checked by a thermocouple. Each spectrum was measured after the sample had been equilibrated for 10 min at an expected temperature. For each case, three independent CD measurements were performed for each protein after the protein was newly prepared, and the representative data were demonstrated.

Thermal-Dependent ATR Infrared Spectroscopy. Attenuated total reflectance (ATR) infrared absorption spectra were recorded at a spectral resolution of 4 cm^{–1} by means of a Bruker vertex 80 v infrared spectrometer equipped with a liquid nitrogen-cooled mercury–cadmium–telluride (MCT) solid-state detector. For the FT-IR measurements, 10 mL containing 0.5 mg/mL of SurF or each deletant, dissolved in the PBS buffer (pH 8.0), was centrifuged in a Amicon Ultra-15 Centrifugal Filter 10 KD (Millipore, Billerica, MA) at 5000 g and 4.0 $^{\circ}$ C and concentrated into a volume of approximately 700 μ L (~7.0 mg/mL). After concentration, the final PBS buffer did not contain 100 mM NaCl and 50 μ M Zn²⁺. The sample compartment was continuously purged with dry air. Then, the protein solution (700 μ L) was injected into the Gateway ATR thermostabilized flow through top-plate assembly with a ZnSe crystal (Specac Inc., Bruker, Germany) controlled through an external water circuit. The measurement was initiated after complete water vapor equilibrium; therefore, the spectral changes observed as a function of

temperature reflect the structural changes due to the thermal transition of the protein and solution H_2O . In the thermal denaturation experiments, the spectra of the protein solution were collected in the temperature range of 30.0–76.0 °C with an increment of 2.0 °C. As for the possible evaporation of the buffer solution in the ATR sample compartment at high temperature and based on the thermal fluorescence profile, no IR spectrum was measured at temperatures above 76.0 °C. Before spectra acquisition, samples were maintained at the desired temperature for 10 min for stabilization of the cell temperature. Spectra of buffer were acquired under the same scanning and temperature conditions. For each spectrum, 128 scans were averaged to ensure a good signal/noise ratio. The temperature was measured with a thermocouple placed in a small bore of the cell window near the sample in order to obtain a precise spectrum–temperature correlation. The series of temperature-dependent spectra were subjected to pretreatments using GRAMS/386 (Thermo Galactic Industries Corporation) to minimize undesirable effects.²⁷ The raw spectra were first truncated between 1700 and 1600 cm^{-1} , and then the contributions of atmospheric water vapor and ectothermic H_2O were subtracted for the removal of the H_2O bending absorption close to 1640 cm^{-1} . After that, the spectra were smoothed with a Gaussian function to reduce the noise and area normalization. Finally, the obtained spectra were baseline corrected in the region of 1700–1600 cm^{-1} . For each case, two independent measurements were performed for each protein after the sample was newly prepared and the representative data were demonstrated.

VV 2D Correlation Analysis. VV 2D correlation contour maps were constructed with a spectral region of 1700–1600 cm^{-1} for the averaged spectra measured at four independent identical conditions and performed according to the method of Noda.^{23,24} To obtain synchronous and asynchronous plots, the 2Dshige program (Shigeaki Morita, Kwansei-Gakuin University, 2004–2005) was used.²⁸ The synchronous plots, covering temperature ranges of 56.0–68.0, 56.0–68.0, 54.0–66.0, and 52.0–64.0 °C were generated for SurF, Sur Δ N7, Sur Δ N13, and Sur Δ N18, respectively. Asynchronous maps were obtained by analyzing the IR absorbance spectra in the identical temperature range for each protein. These temperature ranges were chosen based on the results from CD spectra, which allowed us to better describe the thermal unfolding events.

RESULTS AND DISCUSSION

Tertiary Structural Variations of SurF and the Deletants as Monitored by Fluorescence Spectroscopy. The fluorescence signal of the intrinsic fluorophore, tryptophan residues, is generally very sensitive to polarity and mobility changes of the surrounding environment.^{29,30} As Survivin contains 11 phenylalanine and 3 tryptophan residues (Trp10, Trp25, and Trp67),¹¹ the thermal stabilities of the tertiary structures of SurF and its deletants can be monitored well by temperature-dependent fluorescence spectra (Supporting Information, Figure S2). The emission band centered at 340 nm should be determined mainly by the tryptophan residues contributions, and the intensity of it for SurF and the deletants as a function of temperature (T) is shown in Figure 1. As shown by SurF, the fluorescence intensity at 340 nm decreased with temperature gradually from 30.0 to 56.0 °C, but then, it increased slightly from 58.0 to 60.0 °C and finally decreased again from 62.0 to 84.0 °C. The detected fluorescence changes with temperature reflect mainly the tertiary structural changes of the protein, which reveals that the

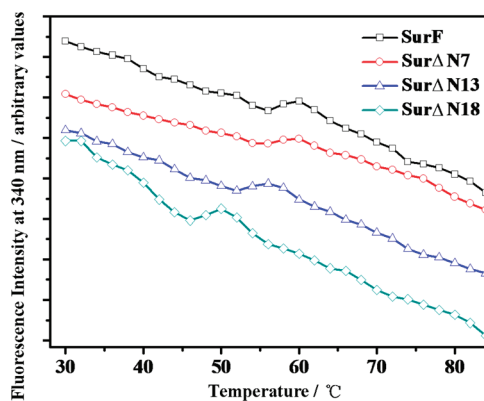


Figure 1. Temperature dependence of the fluorescence variation of the emission at 340 nm: Fluorescence intensities of SurF to Sur Δ N18 at 20 $\mu\text{g}/\text{mL}$ in the PBS buffer including 50 μM Zn^{2+} were recorded at increasing temperatures in the range of 30.0–84.0 °C. The data are representative of three independent experiments.

fluorophore residues, Trp, buried in the native protein have started to become exposed to the solvent before the main unfolding.^{31,32} The decrease of the fluorescence intensity was attributed to the quenching of the exposure of buried fluorophore residues to the aqueous solvent, and the fluorescence increase again was due to an increase in the distance from the fluorophore to the quenchers during the partial unfolding, and then, it continued to decrease until unfolding thoroughly. Similar dependences of the fluorescence emission of other proteins on temperature were also observed previously.^{31–33} The fluorescence intensity profiles revealed large differences of the temperature for partial unfolding between SurF and the deletants (Figure 1), which could be attributed to the possible differences of the tertiary stability between SurF and the deletants. With the N-terminal deletion, the tertiary structural stability degraded, and the protein became more sensitive with temperature. The longer the N-terminal deletion, the less stable the tertiary structure.

In detail, it should be noted that, for the transition temperature, larger differences between Sur Δ N7, Sur Δ N13, and Sur Δ N18 were found, while almost no difference between SurF and Sur Δ N7 was observed. The reason for such differences was directly related to the deletion of N-terminal residues; the results revealed the significant impact of the N-terminal sequence up to Arg18 on the tertiary structural stability of human Survivin in solution. The onset transition temperature of Sur Δ N7 was 56.0 °C, and the completed transition temperature was 60 °C, being almost the same as that of SurF. It was reasonable to observe such result as in Sur Δ N7, all of the main residues that participated in forming the essential hydrophobic pocket were retained except the Leu6,^{8,11,12} which might affect the dimerization strength more or less but not the tertiary structure. However, the deletion up to Pro7 may lead the Trp10 to more solvent exposure and fewer changes with temperature, and it may finally result in a smaller slope of its intensity changes in comparison to that of SurF (Figure 1). A slight decrease of the onset and completed temperatures was observed for Sur Δ N13 versus Sur Δ N7 (52.0 versus 56.0 °C) as all of the N-terminal residues (6–13) previously suggested as being required for dimerization had been removed. Of note was that deletion of the N-terminal sequence up to the conserved Arg18 residues was determined to be important for stabilization of the BIR domain structure, resulted in much lower transition onset and completed

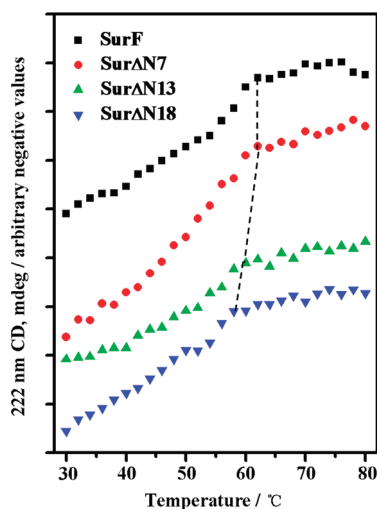


Figure 2. Temperature dependence of the CD spectra variation at 222 nm. SurF to SurΔN18 at 100 $\mu\text{g/mL}$ in PBS buffer, including 50 μM Zn^{2+} , were recorded at increasing temperatures in the range of 30.0 to 80.0 $^{\circ}\text{C}$. SurF was soluble in the supernatant solution, and the deletants were renaturated by dialyses after extraction from inclusion bodies. The data are representative of three independent experiments. The vertical dashed line is to show the changing tendency, that is, the down-shift of transition temperatures from SurF to SurΔN18.

temperatures of 46 and 50 $^{\circ}\text{C}$, and suggested that this protein was very unstable in solution because it was potentially without an intact and incompact BIR domain. In the NMR revealed structure of the Survivin dimer, residues 14–18 were shown to be greatly influenced by the BIR domain and, furthermore, the stability of the tertiary structure.³⁴

In the SMFS experiments, the dimeric unbinding forces between two monomers of SurΔN13 and SurΔN18 were almost the same, but both decreased much more than SurF.²⁵ However, the transition temperature of SurΔN13 was close to those of SurF and SurΔN7, being compared with SurΔN18, which demonstrated that the N-terminal residues up to Phe13 influence the unbinding force of dimerization, but it is not very necessary to keep the tertiary structure. However, the slightly lower transition temperature of SurΔN13 reflected that the dimerization was one factor of influence on the tertiary stability, and according to the SMFS results of SurΔN18, we may know that the N-terminal residues 14–18 did not participate in the dimerization, but they may be very essential for maintaining the BIR domain and the tertiary structure of human Survivin.

Thermal Unfolding of SurF and the Deletants as Monitored by CD Spectroscopy. Both crystallographic diffraction and NMR spectroscopy in solution studies of human Survivin confirmed that the monomer has a long amphipathic C-terminal coiled-coil α -helix (L98–D142) and the BIR domain is composed of a three-stranded antiparallel β -sheet packed against four short α -helices and is stabilized globally by a Zn^{2+} tetrahedrally coordinated by Cys57, Cys60, His77, and Cys84.^{8,11,12} Furthermore, the linker segment forms a short β -sheet. Spontaneous folding of purified SurF and the dialyzed deletants was confirmed by far-UV CD spectra in our previous report.²⁵ The CD spectrum of each protein exhibited double minima at 208 and 222 nm and a positive peak tendency at 195 nm, indicative predominantly of an α -helical secondary structure and consistent with the known crystallographic structural features of the protein

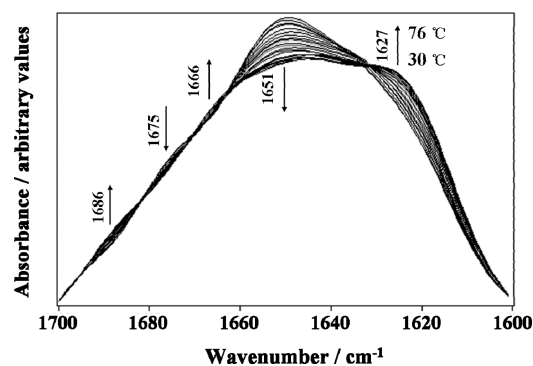


Figure 3. The pretreated temperature-dependent FT-IR spectra of the amide I region of SurF in aqueous solution measured from 30.0 to 76.0 $^{\circ}\text{C}$ with an increment of 2.0 $^{\circ}\text{C}$. The ordinate axis reports the arbitrary units for absorbance spectra.

(see Supporting Information, Figure S3). The 222 nm molar ellipticity of SurF and the deletants as a function of temperature (T) are shown in Figure 2. Under the same conditions, the increases in the 222 nm amplitude of the four proteins were completed at 62.0, 62.0, 60.0, and 58.0 $^{\circ}\text{C}$ from SurF to SurΔN18, respectively. As exemplified by SurF, the 222 nm molar ellipticity increased with temperature gradually from 30.0 to 62.0 $^{\circ}\text{C}$, but then, it remained almost constant from 62.0 to 80.0 $^{\circ}\text{C}$. Therefore, the main transition in secondary structure was assigned at 62.0 $^{\circ}\text{C}$ involved in the main unfolding of SurF and the complete loss of native secondary structures. The transition temperatures revealed here were a little bit higher than those revealed by the intrinsic fluorescence spectroscopy as above, which is quite reasonable as the fluorescence spectral variation is generally the illustration of the tertiary structural changes induced by partial unfolding. Identical operation for the Survivin deletants revealed a similar thermal pathway of SurΔN7, SurΔN13, and SurΔN18, which show main transition temperatures at 62.0, 60.0, and 58.0 $^{\circ}\text{C}$, respectively. Of note is that, it seems that no large difference existed for secondary structural stability between SurF and its deletants. Further evidence will be supplied by the thermal-dependent infrared studies, as illustrated as follows.

Temperature Dependences of the Amide I Band in FT-IR Spectra of SurF and the Deletants. IR absorbance spectra of SurF in aqueous solution were measured between 30.0 and 76.0 $^{\circ}\text{C}$ with an increment of 2.0 $^{\circ}\text{C}$, and those of amide I bands in the region of 1700–1600 cm^{-1} are depicted in Figure 3. The amide I region contains information mainly on the secondary structure of the protein.³⁵ The IR spectrum of SurF at 30.0 $^{\circ}\text{C}$ shows an intense band at 1651 cm^{-1} , which indicates the dominance of α -helix in the native state.³⁶ After deconvolution (see Supporting Information, Figure S4), weak bands at 1627, 1675, and 1686 cm^{-1} can be observed more clearly. The band at 1627 cm^{-1} is typically assigned to the β -sheet structure of the protein.³⁷ The minor bands at 1675 cm^{-1} may contain information on β -sheet structures, while that at 1686 cm^{-1} might be assigned to the β -sheet also. It was noteworthy that this band assignment was less certain because peptide bonds for β -turns were often located in the same region.³⁸ These findings were roughly in agreement with the secondary structural content determined from both the X-ray crystal diffraction and NMR spectroscopy results of full-length human Survivin in solution.^{8,11,12} With the temperature increase, one could observe enormous changes in the intensity of the bands at 1651 and 1627 cm^{-1} ; the amide

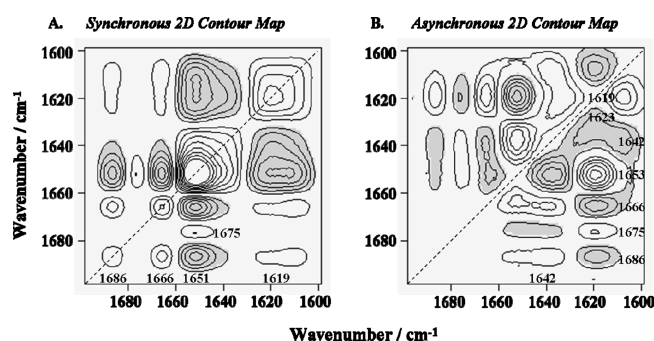


Figure 4. Synchronous (A) and asynchronous (B) 2D contour maps for SurF in the 1700–1600 cm^{-1} region, which are constructed from FT-IR spectra measured under temperature of 56.0–68.0 $^{\circ}\text{C}$. White and gray spots represent positive and negative peaks, respectively. Multiple lines in the maps reflect the intensity of the correlation peaks.

I band underwent a clear red shift of the band maximum, and the shape of the band became broader, characteristic of the protein in the unfolded state. The increasing band at 1627 cm^{-1} was attributed to the gain of β -structures, and therefore, the band shifts observed in amide I provide a direct measurement of the protein unfolding. However, detailed thermal dynamics of SurF cannot be provided clearly in the IR spectra of Figure 3. Improved analytical methods needed to be addressed to reveal more distinct structural variations in response to the thermal perturbation.

Structural Variations in the Main Unfolding of SurF and the Deletants as Revealed by VV 2D Correlation Analysis. By using HPLC, we have found that the N-terminal deletants up to Arg18 of human Survivin were still dimerized in solution,²⁵ and the fluorescence profiles displayed above did show the differences of the tertiary structural kinetics between SurF and the deletants. Furthermore, the transition points of the main transition of the secondary structures were defined through the 222 nm molar ellipticity of far-UV CD spectrum. Therefore, the mechanism needed to be clarified by a more detailed investigation, and it was intriguing to see the secondary structural changes of SurF and the deletants in unfolding by using VV 2D correlation analysis. To provide a better understanding of the secondary conformational changes involved in the unfolding of SurF, the temperature range (56.0–68.0 $^{\circ}\text{C}$) around transition point of denaturation at $T_m = 62.0$ $^{\circ}\text{C}$ was defined based on the temperature-dependent 222 nm molar ellipticity profile of CD spectra (Figure 2). Identical protocols were also performed for the deletants, that is, the stages classified as “major unfolding” were used for the VV 2D analysis for each deletant independently.

Synchronous and asynchronous VV 2D correlation contour maps of dynamic spectral intensity variations induced by temperatures of 56.0–68.0 $^{\circ}\text{C}$ are depicted in Figure 4A and B. They represent the overall extent of the intensity changes caused by this temperature range and demonstrate more a number of well-resolved bands barely identified in the original spectra. In addition to the major autopeak at 1651 cm^{-1} , three other peaks at 1686, 1666, and 1619 cm^{-1} are observed in Figure 4A. The appearance of these autopeaks means that the intensities of these amide bands change significantly with the temperature increase. Prominent autopeaks observed at 1651 cm^{-1} in Figure 4A correspond to the α -helix.³⁹ The contribution of the α -helix structure with an absorption band centered at 1651 cm^{-1} did deconvolute well in the synchronous spectrum, coincidence with its high total content ($\sim 46.3\%$) in native human Survivin.²⁵ The

peaks at 1675 and 1666 cm^{-1} were assigned to the β -sheet and β -turn structures, respectively, which should correspond to the bands observed at 1675 and 1666 cm^{-1} in Figure 3, and substantiated the doubt there to the band assignment; the peak at 1686 cm^{-1} should arise from the β -sheet structure. Of note is that, instead of 1627 cm^{-1} , two newly appearing band at 1623 and 1619 cm^{-1} are observed in Figure 4A, which illustrates the true variations of these two elements over the selected temperature range. The negative cross peaks between 1651 and 1686, 1666, 1623, and 1619 cm^{-1} in Figure 4A suggest that the intensity at 1651 cm^{-1} changed in the opposite direction compare to that of the four bands, while the positive cross peaks at (1666, 1686), (1651, 1675), (1619, 1686), and (1619, 1666) cm^{-1} suggested that the intensity changes of each pair varied in the identical direction with temperature. All of these results indicated the loss of the α -helix (1651 cm^{-1}) and β -sheet (1675 cm^{-1}); meanwhile, the gain of the β -turn- (1666 cm^{-1}) and β -sheet-rich aggregates (1619 cm^{-1}) occurred during the protein unfolding.

Compared with the synchronous spectrum, absorption bands characteristic of various subsecondary and secondary structures in the amide I region were more clearly separated in the asynchronous 2D contour map (Figure 4B), and one could deduce the differences in the thermal stability of secondary structural elements; the peak at 1651 cm^{-1} was separated into two peaks at 1653 and 1642 cm^{-1} , respectively, which were assigned to the α -helix and irregular structures and indicates the formation of a small quantity of random coil during protein unfolding. Of note was that the peak that appeared at 1619 cm^{-1} in the synchronous spectrum was also shown in Figure 4B, being the counterpart of β -sheet-rich aggregates at 1683 cm^{-1} , which may have overlapped the middle-scaled band at 1686 cm^{-1} for the β -sheet structure. In addition, the newly appearing band at around 1607 cm^{-1} was due to the tryptophane (or phenylalanine) side-chain absorption,⁴⁰ which was deconvoluted only in the asynchronous spectrum.

The positive cross peaks at (1619, 1653), (1619, 1675), (1642, 1666) and (1642, 1686) cm^{-1} and the negative cross peaks at (1623, 1642), (1619, 1666), (1619, 1686), (1642, 1653), and (1642, 1675) cm^{-1} could be observed clearly in Figure 4B.

A similar phenomenon could be observed in the temperature-dependent 2D IR spectra of the deletants through the extracted power spectra. The power spectrum along the diagonal line of the synchronous spectrum for each protein is presented in Figure 5. The sequence reveals that the secondary structural variations in the intensity occurred for the bands all due to β -sheet structures (1686, 1675 cm^{-1}) and the β -turn component (1666 cm^{-1}) first and then shifted to the loss of the α -helix (1653 cm^{-1}) and the gain of the β -sheet, that is, the aggregates (1619 cm^{-1}), and finally to the formation of an irregular structure (1642 cm^{-1}). Here, it was shown that the main unfolding of SurF or the N-terminal deletants was initiated with the structural changes of the more temperature-sensitive β -structures and α -helix, followed by the formation of β -sheet-rich aggregates and random coil. Furthermore, the comparison of power spectra in Figure 5 indicated that the content of 1619 cm^{-1} became more extensive with the longer N-terminus deletion. It could be concluded that in the main unfolding, the lower stability of the protein rendered it prone to aggregation with more N-terminal residue deletion.

Thermally Induced Unfolding of SurF and the Deletants.

The IR spectra of SurF (Figure 3) indicated that before 62.0 $^{\circ}\text{C}$, the intensity of the main α -helix band decreased significantly and a new band at around 1627 cm^{-1} appeared, indicating thermal

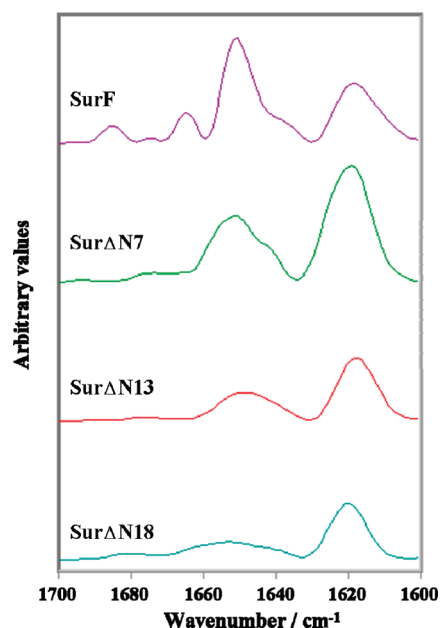


Figure 5. Power spectra extracted from the synchronous 2D contour map of SurF and the deletants in the range of 1700–1600 cm^{-1} .

denaturation and protein unfolding,^{41,42} and similar phenomena were also observed for the three deletants. The analysis of their fluorescence spectra (Figure 1) indicated that the tertiary structural organizations of the deletants were less thermostable than SurF. The X-ray crystal and NMR structural analysis of Survivin and other IAPs illustrated that the Arg18 aliphatic side chain formed a hydrophobic area by packing with residues Ile44 and Phe58;⁸ the hydrogen of the guanidino group, which packed against a pair of aromatic residues, Phe43 and Phe58, was consistently subjected to form a hydrogen bond with the backbone carbonyl oxygen (CO) of Pro12 and Ala39.^{34,43} Furthermore, the positively charged side chain of Arg18 can form attractive cation– π interactions with the aromatic groups,³⁴ and these interactions conserved in a majority of BIR sequences are of significance for the folding of the human Survivin. Therefore, with the removal of the N-terminus, the thermal stability of the tertiary structure dropped vigorously, especially for SurΔN18. However, the secondary structures of the Survivin deletants were not affected very much by the delicate interaction in the fore-mentioned intramolecule.

In the previous work,²⁵ we had quantitatively evaluated the contribution of the N-terminal sequences to the strength of the dimerization by using SMFS first of all and the binding ability to Smac/DIABLO in vitro. However, those experimental results could not explain why the dimeric unbinding force of SurΔN18 was similar to that of SurΔN13 and not much lower than that of SurF but thoroughly lost the binding ability to Smac/DIABLO. As residues 1–18 did not contain the binding site to Smac/DIABLO,³⁴ we presumed that the differences of the structural stability, especially for SurΔN18, may be involved. The investigations of thermal stability for SurF and the deletants confirmed the assumption. By using fluorescence, CD, and infrared spectroscopy, we have demonstrated the mechanism of the thermally induced unfolding pathway and the related structural variations of SurF and the deletants in buffer solutions. Especially, by the extensive use of VV 2D correlation spectroscopy, both the drastic

and subtle structural variations of the main unfolding of SurF and the deletants have been characterized clearly, with temperature, very similar secondary conformational changes with slight differences of aggregation were revealed between SurF and the deletants by the power spectrum. It is reasonable that the N-terminal residues might influence the tertiary structure but not the secondary one which formed normally, but more aggregates were formed for the longer N-terminal deletants during the main unfolding.

CONCLUSIONS

Survivin exists as a homodimer both in solution and in the antiapoptosis state. It is overexpressed in most human neoplasms and becomes an attractive target for cancer therapy. We have determined that the N-terminal sequences up to Arg18 were essential for the dimeric molecule stability. The mechanism of the thermally induced unfolding and the related structural variations have been clarified by the combined use of fluorescence, CD, FT-IR spectroscopy, and especially the 2D correlation analysis. In conclusion, in the main unfolding of the structural changes, the ordered α -helix in SurF and the deletants dominates this process, followed by the structural changes of more temperature sensitive β -structures and the formation of the β -sheet-rich aggregates and random coils. The results obtained from VV 2D correlation analysis further demonstrated the quantitative structural changes of the thermally induced main unfolding; with temperature, very similar secondary conformational changes with slight differences of aggregation were revealed between SurF and the deletants. It could be concluded that the N-terminal residues might influence the tertiary structure but not the secondary ones, although more aggregates were formed for the longer N-terminal deletants during the main unfolding. This study revealed the importance of the N-terminal residues to the thermal stability of human Survivin, which will provide us with new insights into the mechanical properties of human Survivin.

ASSOCIATED CONTENT

S Supporting Information. The coomassie-stained SDS-PAGE electrophoresis gels of SurF and the deletants purified with different pH from the inclusion. The temperature-dependent fluorescence and CD spectra after smoothing by software Origin 7.5. The deconvoluted FT-IR spectra of SurF as a function of temperature at an increment of 2.0 $^{\circ}\text{C}$. This material is available free of charge via the Internet at <http://pubs.acs.org>.

AUTHOR INFORMATION

Corresponding Author

*Fax: +86-431-85193421. Tel: +86-431-85168730. E-mail: yqwu@jlu.edu.cn.

ACKNOWLEDGMENT

The present work was supported by the projects of the Natural Science Foundation of China (Nos. 20934002 and 20973073), Jilin Province Natural Science Foundation (20070926-01), the National Basic Research Program (2007CB808006), the 111 Project (B06009), and the State Key Laboratory for Supramolecular Structure and Materials, Jilin University.

■ REFERENCES

- (1) Altieri, D. C. *Oncogene* **2003**, *22*, 8581.
- (2) Wheatley, S. P.; McNeish, A. *Int. Rev. Cytol.* **2005**, *247*, 35.
- (3) Fukuda, S.; Pelus, L. M. *Mol. Cancer Ther.* **2006**, *5*, 1087.
- (4) Duffy, M. J.; O'Donovan, N.; Brennan, D. J.; Gallagher, W. M.; Ryan, B. M. *Cancer Lett.* **2007**, *249*, 49.
- (5) Mita, A. C.; Mita, M. M.; Nawrocki, S. T.; Giles, F. J. *Clin. Cancer Res.* **2008**, *14*, 5000.
- (6) Pennati, M.; Folini, M.; Zaffaroni, N. *Expert Opin. Ther. Targets* **2008**, *12*, 463.
- (7) Capalbo, G.; Rodel, C.; Stauber, R. H.; Knauer, S. K.; Bache, M.; Kappler, M.; Rodel, F. *Strahlenther. Onkol.* **2007**, *183*, 593.
- (8) Chantalat, L.; Skoufias, D. A.; Kleman, J. P.; Jung, B.; Dideberg, O.; Margolis, R. L. *Mol. Cell* **2000**, *6*, 183.
- (9) Sun, C. H.; Cai, M. L.; Meadows, R. P.; Xu, N.; Gunasekera, A. H.; Herrmann, J.; Wu, J. C.; Fesik, S. W. *J. Biol. Chem.* **2000**, *275*, 33777.
- (10) Bourhis, E.; Hymowitz, S. G.; Cochran, A. G. *J. Biol. Chem.* **2007**, *282*, 35018.
- (11) Verdecia, M. A.; Huang, H. K.; Dutil, E.; Kaiser, D. A.; Hunter, T.; Noel, J. P. *Nat. Struct. Biol.* **2000**, *7*, 602.
- (12) Sun, C. H.; Nettesheim, D.; Liu, Z. H.; Olejniczak, E. T. *Biochemistry* **2005**, *44*, 11.
- (13) Lens, S. M. A.; Vader, G.; Medema, R. H. *Curr. Opin. Cell Biol.* **2006**, *18*, 616.
- (14) Jeyaprakash, A. A.; Klein, U. R.; Lindner, D.; Ebert, J.; Nigg, E. A.; Conti, E. *Cell* **2007**, *131*, 271.
- (15) Forman, J. R.; Clarke, J. *Curr. Opin. Struct. Biol.* **2007**, *17*, 58.
- (16) Santucci, R.; Sinibaldi, F.; Fiorucci, L. *Mini Rev. Med. Chem.* **2008**, *8*, 57.
- (17) Levitsky, D. I.; Pivovarova, A. V.; Mikhailova, V. V.; Nikolaeva, O. P. *FEBS J.* **2008**, *275*, 4280.
- (18) Gao, Y. S.; Su, J. T.; Yan, Y. B. *Int. J. Mol. Sci.* **2010**, *11*, 2584.
- (19) Mukherjee, S.; Waagele, M. M.; Chowshury, P.; Guo, L.; Gai, F. *J. Mol. Biol.* **2009**, *393*, 227.
- (20) Ozaki, Y.; Noda, I. *Two-dimensional correlation spectroscopy*; Kobe-Sanda: Japan, August–September 1999; American Institute of Physics: Melville, NY, 2000.
- (21) Noda, I.; Ozaki, Y. *Two-dimensional correlation spectroscopy: applications in vibrational and optical spectroscopy*; John Wiley & Sons: Chichester, West Sussex, England; Hoboken, NJ, 2004.
- (22) Noda, I. *Appl. Spectrosc.* **1990**, *44*, 550.
- (23) Noda, I. *Appl. Spectrosc.* **1993**, *47*, 1329.
- (24) Noda, I.; Dowrey, A. E.; Marcott, C.; Story, G. M.; Ozaki, Y. *Appl. Spectrosc.* **2000**, *54*, 236a.
- (25) Gao, Y.; Zhang, H.; Zhang, M.; Zhang, H.; Yu, X.; Kong, W.; Zha, X.; Wu, Y. *J. Phys. Chem. B* **2010**, *114*, 15656.
- (26) Li, C.; Wu, Z.; Liu, M.; Pazgier, M.; Lu, W. *Protein Sci.* **2008**, *17*, 1624.
- (27) Czarnik-Matusiewicz, B.; Murayama, K.; Wu, Y. Q.; Ozaki, Y. *J. Phys. Chem. B* **2000**, *104*, 7803.
- (28) Morita, S.; Shinzawa, H.; Noda, I.; Ozaki, Y. *Appl. Spectrosc.* **2006**, *60*, 398.
- (29) Nienhaus, G. U.; Wiedenmann, J. *ChemPhysChem* **2009**, *10*, 1369.
- (30) Fitter, J. *Cell. Mol. Life Sci.* **2009**, *66*, 1672.
- (31) van Mierlo, C. P. M.; Steensma, E. J. *Biotechnol.* **2000**, *79*, 281.
- (32) Guzzi, R.; Sportelli, L.; Sato, K.; Cannistraro, S.; Dennison, C. *Biochim. Biophys. Acta, Proteins Proteomics* **2008**, *1784*, 1997.
- (33) Wang, L. X.; Wu, Y. Q.; Meersman, F. *Vib. Spectrosc.* **2006**, *42*, 201.
- (34) Luque, L. E.; Grape, K. P.; Junker, M. *Biochemistry* **2002**, *41*, 13663.
- (35) Arrondo, J. L.; Muga, A.; Castresana, J.; Goni, F. M. *Prog. Biophys. Mol. Biol.* **1993**, *59*, 23.
- (36) Torrent, J.; Rubens, P.; Ribo, M.; Heremans, K.; Vilanova, M. *Protein Sci.* **2001**, *10*, 725.
- (37) Meersman, F.; Heremans, K. *Biophys. Chem.* **2003**, *104*, 297.
- (38) Krimm, S.; Bandekar, J. *Adv. Protein Chem.* **1986**, *38*, 181.
- (39) Marabotti, A.; Scire, A.; Staiano, M.; Crescenzo, R.; Aurilla, V.; Tanfani, F.; D'Auria, S. *J. Proteome Res.* **2008**, *7*, 5221.
- (40) Barth, A. *Biochim. Biophys. Acta* **2007**, *1767*, 1073.
- (41) Ausili, A.; Cobucci-Ponzano, B.; Di Lauro, B.; D'Avino, R.; Perugino, G.; Bertoli, E.; Scire, A.; Rossi, M.; Tanfani, F.; Moracci, M. *Proteins* **2007**, *67*, 991.
- (42) Meersman, F.; Heremans, K. *Biochemistry* **2003**, *42*, 14234.
- (43) Song, Z. Y.; Yao, X. B.; Wu, M. J. *J. Biol. Chem.* **2003**, *278*, 23130.